CJST *Caribbean Journal of Science and Technology*, **2022**, *10(1)*, 36-42

Research Article

Carib. J. Sci. Tech.

Investigation of Torsional Vibrations in Magnetic Field Poroelastic Hollow Cylinders

Manjula Ramagiri*

Article DOI:
10.55434/CBI.2022.10106

Author's Affiliations

Department of Mathematics
University Arts and Science College (Autonomous)
Kakatiya University
Warangal-506009, Telangana, INDIA.

Corresponding Author

Manjula Ramagiri
manjularamagiri@gmail.com

Received- 23rd June 2022,
Provisional Acceptance- 30th June 2022

ISSN 0799-3757

http://caribjscitech.com/

Abstract

Investigations are made into how the magnetic field affects torsional vibrations in poroelastic hollow cylinders. When the boundaries have free, fixed, and mixed boundary conditions, the frequency equation is explored. Most of the equations have been taken from Biot,s theory. Governing equations are derived in the presence of magnetic field. It is demonstrated that the magnetic field in poroelastic cylinders has a considerable impact on the dispersion curves. The theoretically obtained results are computed and graphically displayed.

Keywords: Poroelasticity; Magnetic field; Frequency equation; Phase velocity; Hollow cylinder; Torsional vibrations

Introduction

Torsional vibrations are important in cylinder engines, and/or in the engines working at high rotational speeds. These types of enginesaredangerous in the range of operating rotational speed. As a result, the input frequency can get close to the torsional natural frequency of the shaft. Magnetoelastic torsional waves in a bar under initial stress are discussed in[1]. In the current study, they firstly discussed when rods are homogeneous & thereafter when they aren't homogeneous. Torsional vibrations of circular elastic plates with thickness steps are investigated in[2]. In[3] authors investigated the torsional wave propagation in hollow cylindrical bars. In the said paper torsion wave propagation is presented for both solid rods and hollow cylindrical rods of various geometries. Trapped torsional vibrations in elastic plates are investigated in[4]. In[5], scientists examined magneto-elastic torsional waves in an initial-stressed composite, non-homogeneous cylindrical shell. In[6], the authors investigated the natural vibrational frequencies of a hollow magnetoelastic cylinder subjected to substantial deformation.

Torsional vibrations of a finite hollow poroelastic circular cylinder are examined in[7] using Biot's theory[8]. The torsional vibration in infinite hollowed poroelastic cylinders were investigated by authors of[9]. Presents[10] vibrations due to torsion therein the poroelastic dissipative hollow thick-walled cylinder with a starting tension. discusses coated hollow poroelastic spheres' torsional vibrations. Using[11] the extension theory, authors in[12] explored torsional vibrations in thick-walled, hollow poroelastic cylinders. Studied[13] composite poroelastic spherical shell-extension biot's theory torsional vibrations.Within the context of Biot viscosity-extended theory, authors reported torsional waves of infinite fully saturated poroelastic cylinders in[14]. Discusses[15] the torsional vibrations of a fluid-filled multilayered transversely isotropic finite circular cylinder.

Presents[16] a study of radial vibrations in a hollow, isotropic, poroelastic cylinder with biot/squirt (BISQ) media. Investigates[17] torsional wave propagation due to torsion therein hollow poro-thermo-elastic cylinder. The magnetic field is not taken into account in the fore mentioned works when torsional vibrations for poroelasticity. The effect of a magnetic field on vibrations due to torsion in poroelastic hollow cylinders is discussed in the current work. For two different types of cylinders, frequency versus ratio of thickness to inner radius is estimated.

Governing equations and solution of the problem

Let (r,θ,z) represent the cylindrical polar coordinates. Consider a homogenous, isotropic hollow poroelastic cylinder with a z-axis-directed axis and radii of a and b, respectively. The motion equations are provided in[7]:

$$\frac{\partial\sigma_{rr}}{\partial r}+\frac{1}{r}\frac{\partial\sigma_{r\theta}}{\partial\theta}+\frac{\partial\sigma_{rz}}{\partial z}+\frac{\sigma_{rr}-\sigma_{\theta\theta}}{r}+F_r=\frac{\partial^2}{\partial t^2}(\rho_{11}u+\rho_{12}U),$$
$$\frac{\partial\sigma_{\theta r}}{\partial r}+\frac{1}{r}\frac{\partial\sigma_{\theta\theta}}{\partial\theta}+\frac{\partial\sigma_{\theta z}}{\partial z}+\frac{2\sigma_{r\theta}}{r}+F_\theta=\frac{\partial^2}{\partial t^2}(\rho_{11}v+\rho_{12}V),$$
$$\frac{\partial\sigma_{zr}}{\partial r}+\frac{1}{r}\frac{\partial\sigma_{z\theta}}{\partial\theta}+\frac{\partial\sigma'_{zz}}{\partial z}+\frac{\sigma_{rz}}{r}+F_z=\frac{\partial^2}{\partial t^2}(\rho_{11}w+\rho_{12}W),$$

$$\frac{\partial s}{\partial r}=\frac{\partial^2}{\partial t^2}(\rho_{12}u+\rho_{22}U),$$

$$\frac{1}{r}\frac{\partial s}{\partial\theta}=\frac{\partial^2}{\partial t^2}(\rho_{12}v+\rho_{22}V),$$

$$\frac{\partial s}{\partial z}=\frac{\partial^2}{\partial t^2}(\rho_{12}w+\rho_{22}W). \tag{1}$$

Where, solid displacements are denoted by $\vec{u}(u,v,w)$ and fluid displacements by $\vec{U}(U,V,W)$ are. ρ_{ij} - mass coefficients. $\sigma_{rr},\sigma_{\theta\theta},\sigma_{zz},\sigma_{rz},\sigma_{r\theta},\sigma_{\theta z}$ - stresses components and fluid pressure - s. $F=(F_r,F_\theta,F_z)$ are the Lorentz force because of axial magnetic field is[1]

$$F=J\times B \tag{2}$$

Stress components σ_{ij} and fluid pressure [7] are expressed as

$$\sigma_{ij}=2Ne_{ij}+(Ae+Q\varepsilon)\delta_{ij} \qquad (i,j=r,\theta,z),$$
$$s=Qe+R\varepsilon. \tag{3}$$

In eq. (3), e_{ij}'s strain displacements, σ_{ij}'s are solid stresses and fluid pressure s, δ_{ij} the well-known Kroneckar delta function. e is the solid dilatation and ε is the fluid dilatation. The constants of poro-elasticity are given by the notations A, N, Q, R. Maxwell equations governing, electromagnetic fields on solid medium having electrical conductivity are[1]

$$curlH=4\pi J,\quad curlE=\frac{-1}{c}\frac{\partial B}{\partial t},\quad divB=0,\quad B=\mu_e H \tag{4}$$

Where, displacement current is neglected and as per ohm's law

$$J=\sigma(E+\frac{1}{c}\frac{\partial u}{\partial t}\times B) \tag{5}$$

Equations (4) and (5), H,B,E,J represent the vectors of magnetic intensity, magnetic induction, electric intensity, and current density; μ_e,σ,u represent the vectors of magnetic permeability, electrical conductivity, and displacement in the strained state, respectively; and c represents the speed of light. The vacuum equations for the electromagnetic field are [1].

$$(\nabla^2-\frac{1}{c^2}\frac{\partial^2}{\partial t^2})E^*=0,(\nabla^2-\frac{1}{c^2}\frac{\partial^2}{\partial t^2})h^*=0,$$
$$CurlE^*=-\frac{1}{c}\frac{\partial h^*}{\partial t},Curlh^*=\frac{1}{c}\frac{\partial E^*}{\partial t}. \tag{6}$$

Where, h^* perturbation magnetic field in the vacuum. E^* - electric field in the vacuum. Now let suppose that $H=H_0+h$, where H_0 initial magnetic field. h small perturbation within the region. Suppose the cylinder is a good conductor of electricity (i.e, $\sigma\to\infty$) hence eqn. (5) provides

$$E=\frac{-1}{c}\frac{\partial u}{\partial t}\times B=(\frac{-H}{c}\frac{\partial v}{\partial t},0,0) \tag{7}$$

Where, $H=|H_0|$. Eliminating E from eq. (4) and eq. (7) we obtain

$$h=(0,H\frac{\partial v}{\partial z},0) \tag{8}$$

From eq. (4) and eq. (8) we get

$$J\times B=J\times\mu_e H_0=(0,\frac{-H^2}{4\pi}\frac{\partial^2 v}{\partial z^2},0)$$

(9)

For vibrations due to torsion, equations of motion is reduced to

$$\frac{\partial\sigma_{\theta r}}{\partial r}+\frac{\partial\sigma_{\theta z}}{\partial z}+\frac{2\sigma_{r\theta}}{r}-\frac{H^2}{4\pi}\frac{\partial^2 v}{\partial z^2}=\frac{\partial^2}{\partial t^2}(\rho_{11}v+\rho_{12}V),$$
$$0=\frac{\partial^2}{\partial t^2}(\rho_{12}v+\rho_{22}V).$$

(10)

Assume that the harmonic wave solution takes the following form

$$v(r)=v_1(r)e^{ik(z-\omega t)},$$
$$V(r)=V_1(r)e^{ik(z-\omega t)}.$$

(11)

In eq. (11) ω is the frequency, k - the wavenumber, and t - time. Substituting eq. (11) and eq. (3) in eq. (10), one obtains

$$N\frac{d^2v_1}{dr^2}+\frac{N}{r}\frac{dv_1}{dr}-N\frac{v_1}{r^2}-k^2(1-\frac{H^2}{4N\pi})v_1=-\omega^2(\rho_{11}v_1+\rho_{12}V_1),$$
$$0=-\omega^2(\rho_{12}v_1+\rho_{22}V_1)$$

(12)

The general solution of eq. (12) takes the following form

$$v(r)=[AJ_1(pr)+BY_1(pr)]e^{ik(z-\omega t)},$$
$$V(r)=\frac{-\rho_{11}}{\rho_{22}}[AJ_1(pr)+BY_1(pr)]e^{ik(z-\omega t)}.$$

(13)

Where, $p=\frac{\omega^2}{V_s^2}-k^2(1-\frac{H^2}{4\pi N})$. A, B denotes the arbitrary constants and $J_1(pr), Y_1(pr)$ are the first kind Bessel's functions. V_s denotes shear wave velocity [7]. The non -zero stresses are

$$\sigma_{r\theta}=A[NpJ_0(pr)-\frac{2N}{r}J_1(pr)]+B[NpY_0(pr)-\frac{2N}{r}Y_1(pr)].$$

(14)

Boundary conditions and equation of frequency

Free surface traction

In this case, the frequency equation and the boundary conditions demonstrating that the outer and inner surfaces are free.

$$\sigma_{r\theta}=0 \text{ at } r=a \text{ and}$$
$$\sigma_{r\theta}=0 \text{ at } r=b$$

(15)

Using Eqs. (15) and (14), one obtains two homogeneous equations

$$A[NpJ_0(pa)-\frac{2N}{a}J_1(pa)]+B[NpY_0(pa)-\frac{2N}{a}Y_1(pa)]=0,$$
$$A[NpJ_0(pb)-\frac{2N}{b}J_1(pb)]+B[NpY_0(pb)-\frac{2N}{b}Y_1(pb)]=0.$$

(16)

Eliminating the constants one obtain frequency equation as follows

$$\begin{vmatrix} A_{11} & A_{12} \\ A_{21} & A_{22} \end{vmatrix}=0$$

(17)

Where,

$$A_{11}=NpJ_0(pa)-\frac{2N}{a}J_1(pa),\quad A_{12}=NpY_0(pa)-\frac{2N}{a}Y_1(pa),$$
$$A_{21}=NpJ_0(pb)-\frac{2N}{b}J_1(pb),\quad A_{22}=NpY_0(pb)-\frac{2N}{b}Y_1(pb).$$

(18)

Fixed surface

In this instance, the boundary environs shows that inner as well as outer surface are fixed & frequency equation is discussed

$$v(r)=0 \text{ at } r=a \text{ and}$$
$$v(r)=0 \text{ at } r=b$$

(19)

From Eqs. (13) and (19), one obtains twohomogeneous equations

$$AJ_1(pa)+BY_1(pa)=0, \text{and } AJ_1(pb)+BY_1(pb)=0.$$

(20)

Eliminating the constants one obtain frequency equation as follows

$$\begin{vmatrix} B_{11} & B_{12} \\ B_{21} & B_{22} \end{vmatrix}=0$$

(21)

Where,

$$B_{11}=J_1(pa),\ B_{12}=Y_1(pa),\ B_{21}=J_1(pb),\ B_{22}=Y_1(pb).$$

(22)

Inner surface fixed and outer surface free

In this instance, the discussion of frequency equation follows the boundary conditions' definition that inner surface being fixed as well as the outer surface remains free.

$$v(r)=0 \text{ at } r=a \text{ and}$$
$$\sigma_{r\theta}=0 \text{ at } r=b$$

(23)

Two homogenous Eqns are from Eqns (13) (14) and (23)

$$AJ_1(pa)+BY_1(pa)=0, \quad A[NpJ_0(pb)-\frac{2N}{b}J_1(pb)]+B[NpY_0(pb)-\frac{2N}{b}Y_1(pb)]=0 \tag{24}$$

Eliminating the constants one obtain frequency equation as follows

$$\begin{vmatrix} C_{11} & C_{12} \\ C_{21} & C_{22} \end{vmatrix} = 0 \tag{25}$$

Where,

$$C_{11} = J_1(pa), C_{12} = Y_1(pa),$$
$$C_{21} = NpJ_0(pb) - \frac{2N}{b}J_1(pb), \quad C_{22} = NpY_0(pb) - \frac{2N}{b}Y_1(pb). \tag{26}$$

Inner surface free and outer surface fixed

The frequency equation is explained in respect to the boundary conditions here, which state that free inner surface and fixed external surface.

$$\sigma_{r\theta} = 0 \text{ at } r = a \text{ and}$$
$$v(r) = 0 \text{ at } r = b \tag{27}$$

Using eqns. (13), (14) and (27) one obtains two homogeneous equations

$$A[NpJ_0(pa) - \frac{2N}{a}J_1(pa)] + B[NpY_0(pa) - \frac{2N}{a}Y_1(pa)] = 0,$$
$$AJ_1(pb) + BY_1(pb) = 0. \tag{28}$$

Eliminating the constants one obtain frequency equation as follows

$$\begin{vmatrix} D_{11} & D_{12} \\ D_{21} & D_{22} \end{vmatrix} = 0 \tag{29}$$

Where,

$$D_{11} = NpJ_0(pa) - \frac{2N}{a}J_1(pa), \quad D_{12} = NpY_0(pa) - \frac{2N}{a}Y_1(pa)$$
$$D_{21} = J_1(pb), D_{22} = Y_1(pb), \tag{30}$$

Numerical results

The frequency equations (17), (21), (25) and (29) are used to calculate the numerical results. For two different types of cylinders, frequency is computed. Sandstone saturated with water makes up cylinders I [18] and II, sandstone saturated with kerosene [19]. For different magnetic intensities, one can establish an implicit relationship between frequency and the ratio of thickness to inner radius by using the values from the frequency equation (H). Let $g = \frac{b}{a}$ so that $\frac{h_1}{a} = g - 1$. In **Table 1**, the physical characteristics of cylinders are listed.

Table-1

Cylinder-I	Cylinder-II
$N = 0.2765 \times 10^{10} N/m^2$	$N = 0.922 \times 10^{10} N/m^2$
$\rho_{11} = 1.926137 \times 10^3 kg/m^3$	$\rho_{11} = 1.90302 \times 10^3 kg/m^3$
$\rho_{12} = -0.00213 \times 10^3 kg/m^3$	$\rho_{12} = 0$
$\rho_{22} = 0.21537 \times 10^3 kg/m^3$	$\rho_{22} = 0.268 \times 10^3 kg/m^3$

Figure 1 depicts the frequency variation against thickness to inner radius for free traction surface (cylinder-I). **Figure 2** depicts the frequency variation thickness to inner radius for free traction surface (cylinder-II). **Figure 3** displays the frequency fluctuation in relation to the thickness to inner radius for a fixed surface (cylinder-I). Plots of variation versus the thickness-to-inner-radius ratio for fixed surfaces (cylinder-II) are shown in **Figure 4**.

Figure 5 displays the frequency fluctuation versus the thickness to inner radius ratio for the inner fixed surface and the outer free surface for (cylinder-I). **Figure 6** displays the frequency variation versus the thickness to inner radius ratio for the inner fixed surface and the outer free surface for (cylinder-II). **Figure 7** displays the frequency variation versus the thickness to inner radius ratio for the inner surface free and the outer surface fixed for (cylinder-I). **Figure 8** depicts the frequency fluctuation versus the thickness to inner radius ratio for the inner surface free and the outer surface fixed for (cylinder-II). Generally, cylinder-II values are higher than cylinder-I values. It can be seen in all of the figures that frequency decreases as the thickness to inner radius ratio increases. Due to the presence of a magnetic field within the solid portion, cylinder-II frequency is higher than cylinder- I.

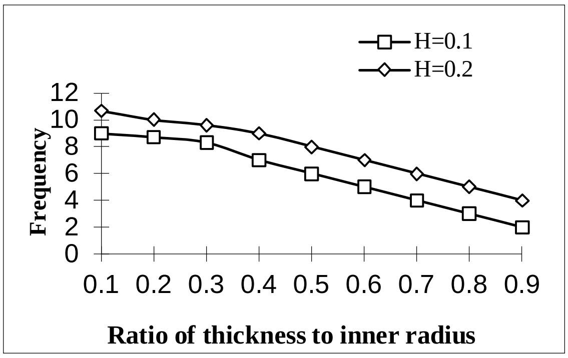

Fig. 1: Frequency v/s ratio of thickness to inner radius for free traction surface (cylinder-I)

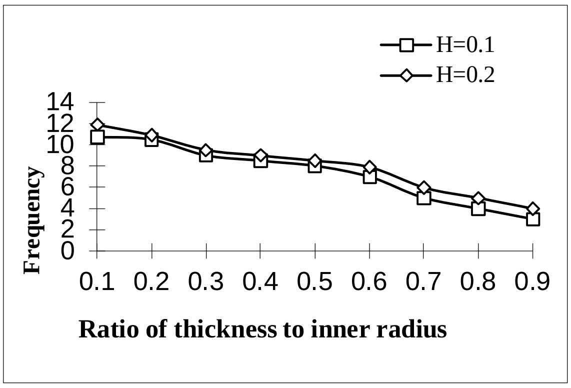

Fig. 2: Frequency V/s ratio of thickness to inner radius for free traction surface (cylinder-II)

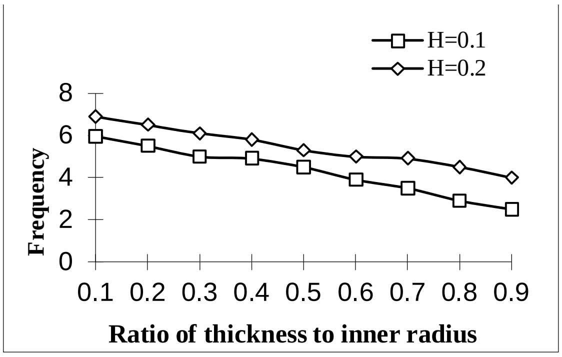

Fig. 3: Frequency v/s ratio of thickness to inner radius for fixed surface (cylinder-I)

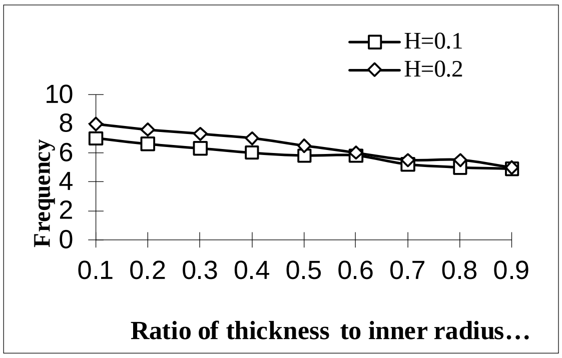

Fig. 4: Frequency v/s ratio of thickness to inner radius for fixed surface (cylinder-II)

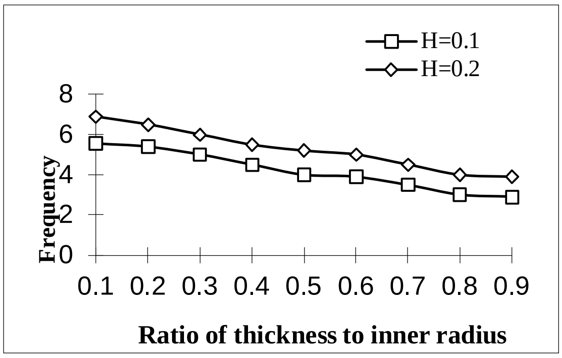

Fig. 5: Frequency v/s thickness to inner radius ratio for fixed inner surface and free outer surface (cylinder-I)

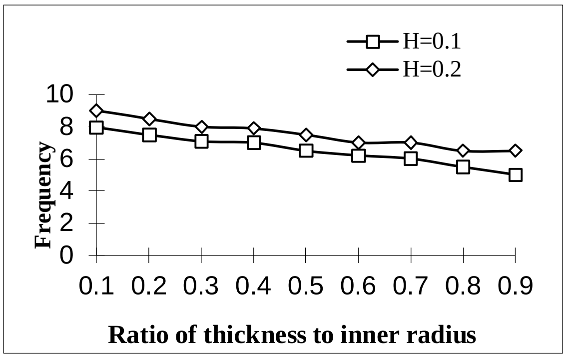

Fig. 6: Frequencyv/s ratio of thickness to inner radius for inner surface fixed and outer surface free(cylinder-II)

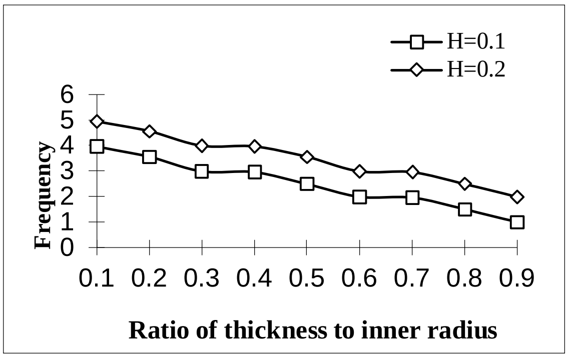

Fig. 7: Frequency v/s thickness ratio to inner radius for free inner surface and fixed outer surface (cylinder-I)

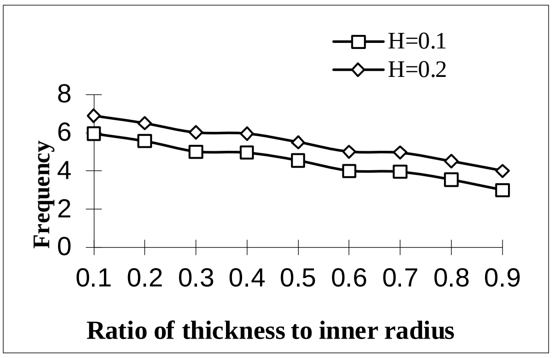

Fig. 8: Frequency v/s thickness ratio to inner radius for free inner surface and fixed outer surface (cylinder-II)

Conclusion

It has been investigated that magnetic field affects a poroelastic hollow cylinder's torsional vibrations. For various surfaces, the frequency equations are derived under the influence of the magnetic field. For various scenarios, the numerical results are obtained and analysed. In every instance, the frequency drops if there is increase in thickness to inner radius ratio increases. The approach described in the research is applied to numerous poroelasticity and elasticity related issues. The mechanical engineering and industrial sectors use these applications.

Nomenclature

σ_{ij} - stresses
$\vec{u}\,(u, v, w)$ - solid displacements
σ_{ij} - stresses
ρ_{ij} - mass coefficients
s fluid pressure
e solid dilatation
ε fluid dilatation
δ_{ij} kroneckar delta function
A, N, Q, R - poroelastic constants
H magnetic intensity
B magnetic induction
E electric intensity
J current density
μ_e magnetic permeability
σ electrical conductivity
c speed of light
H_0 initial magnetic field
H small perturbation
E^* electric field in vaccum
V_s shear wave velocity
ω frequency
k wavenumber
t time

Conflict of Interest

The author declares no conflict of interest on the present work.

Funding Details

No financial assistance to the present work.

References:

1. Surya, N.; *Pro. Indian. Acad. Sci. (Mathematical Sciences-2)*, **1978**, *5*, 137.
2. Min, K.K.; Rui, H.; Terence, K. *IEEE. Tran. on Ultr, Ferro. Freq. Control*. **2006**, *53(2)*, 349. DOI:10.1109/TUFFC.2006.1593373
3. Clark, S. K. *Journal of the Acoustical Society of America*, **1956**, *28*, 1163. DOI: https://doi.org/10.1121/1.1908581
4. Knowles, T.; Min., K.K.; Rui, H. *Applied Physics Letters*, **2005**, *87*, 201911. DOI: http://dx.doi.org/10.1063/1.2131184
5. Surya Narain.; Leena Lahari. *Def. sci. J* .**1981**, *31(2)*, 125132. DOI:https://doi.org/10.14429/dsj.31.6349
6. Olokuntoye, B.; Akinola, A.; Layeni, O.; Fadodun, O. *Int. J. of Eng Res & Tech*. ***2020***, *9(9)*, 328. DOI:10.17577/IJERTV91SO90010
7. Biot, M.A. *Journal of the Acoustical Society of America*, **1956**, *28*, 168. DOI: 10.1121/11908239
8. Tajuddin, Md.; Sarma, K.S.; *Def. Sci. J.* **1978**, *28(2)*, 97.DOI://doi.org/10.14429/dsj.28.6542
9. Tajuddin, M.; Shah, A.S.; *J. Mec. Mat. Stru.* **2007**, *2(1)*, 189-200. DOI:10.2140/jomms.2007.2.189.

10. Balu, Ch.; Ramesh, M.; Sandhya Rani, B.; Malla Reddy, P. *Speci Top and Rev in Porous Media- An Int. J.* **2019**, *10(5)*, 447. DOI:10.1615/special Topics Rev Porous media.2019018980
11. Shah, S.; Nageswaranath, C.; Ramesh, M.; Ramanamurthy, M. *Open J. Acous.*, **2017**, *7(1)*,18-26. DOI: 10.4236/oja.2017.71003
12. Malla Reddy, P.; Rajitha, G. *Sadhana*., **2015**, *40(6)*,1925. DOI: 10.1007/SI2046-015-0395-1
13. Rajitha, G.; Malla Reddy. P; *J. Solid. Mech.* **2020**, *12(3)*, 649. DOI:10.22034/jsm.2020.1885789
14. Solorza-Calderon, S.*App. Math. and Comp*., **2021**, *391*, 125636. DOI: https://doi.org/10.1016/j.amc.2020.125636
15. Abassi, W.; El-Baroundi, A.; Razafimahery, F. *Int. J. App. Mech.*, **2016**, *8(3)*,1650032. DOI:10.1142/S1758825116500320
16. Manjula, R. *Journal of Engineering Sciences(JES).* **2020**, *11(4)*, 1533. DOI: 2020-1104220.pdf (jespublication.com)
17. Manjula Ramagiri.; *Int. J. Mod. Trends Sci. and Techy*, **2019**, *5(6)*, 27. DOI: http://www.ijmtst.com/vol5issue06.html
18. Yew, C.H.; Jogi, P.N.; *Journal of the Acoustical Society of America,* **1976**, *60*, 2. https://doi.org/10.1121/1.381045.
19. Fatt, I. *J. App. Mech*. **1959**, *26(2)*, 296.